Furnace Annealing Behavior of B-doped Poly-SiGe Formed on Insulating Film

Tsunoda, Isao
Department of Electronics, Graduate School of Information Science and Electrical Engineering, Kyushu University : Graduate Student

Sadoh, Taizoh
Department of Electronics, Faculty of Information Science and Electrical Engineering, Kyushu University

Miyao, Masanobu
Department of Electronics, Faculty of Information Science and Electrical Engineering, Kyushu University

https://doi.org/10.15017/1515848

出版情報：九州大学大学院システム情報科学紀要. 8 (2), pp.151-154, 2003-09-26. 九州大学大学院システム情報科学研究院
バージョン：
権利関係：

九州大学大学院
システム情報科学紀要
第8巻 第2号 平成15年9月

Research Reports on Information Science and
Electrical Engineering of Kyushu University
Vol.8, No.2, September 2003

Furnace Annealing Behavior of B-doped Poly-SiGe Formed on Insulating Film

Isao TSUNODA*, Taizoh SADOH** and Masanobu MIYAO**

(Received June 13, 2003)

Abstract: Furnace-annealing behavior of B-doped poly-SiGe on insulating films has been investigated. With increasing Ge fraction, thermal stability of electrically active B atoms at a supersaturated concentration was significantly improved, for example, the stability at 800°C for poly-$Si_{0.6}Ge_{0.4}$ films was nine times as high as that for poly-Si films. The deactivation process consists of the fast and slow processes. The fast process was due to sweeping out of B atoms from substitutional to interstitial sites, enhanced by a local strain induced by the difference in atomic radii between Si and B atoms, and the slow process was due to trapping of B at grain boundaries during grain growth by annealing. The improved thermal stability of B atoms is due to the local strain compensation by Ge doping.

Keywords: Poly-SiGe, Doping, Annealing, MOSFET, ULSI

1. Introduction

Poly-SiGe is a promising material for gate electrodes in the future ultralarge-scale integrated circuits (ULSIs) because of the low resistivity and the ability of work function tuning[1),2),3),4),5),6)].

Doping characteristics and effects of dopant atoms on grain growth in *in-situ* doped poly-SiGe films have been investigated by many researchers[7),8),9)]. However, diffusion and deactivation of dopant atoms can be modulated significantly by the grain boundaries and Ge fraction. Consequently, the thermal stability of dopant atoms should be examined in order to establish the poly-SiGe films as ULSI materials. In line with this, post-annealing behavior of *in-situ* doped poly-SiGe layers on SiON films has been investigated.

2. Experimental Procedures

The SiON films (thickness: 2.5 nm) were grown on Si wafers. Subsequently, Si buffer layers (2 nm) and SiGe layers (70–180 nm) were deposited at 690°C by the reduced pressure chemical vapor deposition (CVD). During deposition, B_2H_6 was introduced into the chamber for *in-situ* doping of B. The flat B profile with the concentration of about 2×10^{20} cm^{-3} was confirmed by SIMS measurements. Finally, the samples were annealed at 600–900°C for 5–5000 min in nitrogen ambient. The carrier density was evaluated by using Hall effect measurements.

* Department of Electronics, Graduate Student
** Department of Electronics

3. Results and Discussion

Post-annealing characteristics of carrier density in *in-situ* B doped poly-SiGe annealed at 800°C are shown in Fig. 1(a). With increasing annealing time, the carrier density decreases and converges to a constant value. The rate of decrease is lower for samples with a higher Ge fraction, which suggests that thermal stability of carriers increases with increasing Ge fraction. The decrease in the carrier density can be attributed to segregation of B at the sample surface or the interface with SiON, or electrical deactivation of B in the poly-SiGe film. The SIMS measurements revealed that the B concentration profiles did not change after post-annealing, *i.e.*, the profiles showed a flat distribution of B atoms with a concentration of about 2×10^{20} cm^{-3} in the SiGe layers (70–180 nm). Thus, it is suggested that the decrease in the carrier density is due to deactivation of B.

Figure 1(b) compares the average carrier concentrations for as-deposited and annealed (10^3 min) samples. The average carrier concentration was obtained by dividing the carrier density by the layer thickness, assuming that carriers were distributed uniformly in the depth direction. The thermal equilibrium solubility of B in SiGe[9)] is also shown as a function of the Ge fraction in Fig. 1(b). The results suggest that the decrease in the carrier concentration after post-annealing is due to a transition from the supersaturated concentration in the as-deposited films to the thermal equilibrium solubility of B at the annealing temperature.

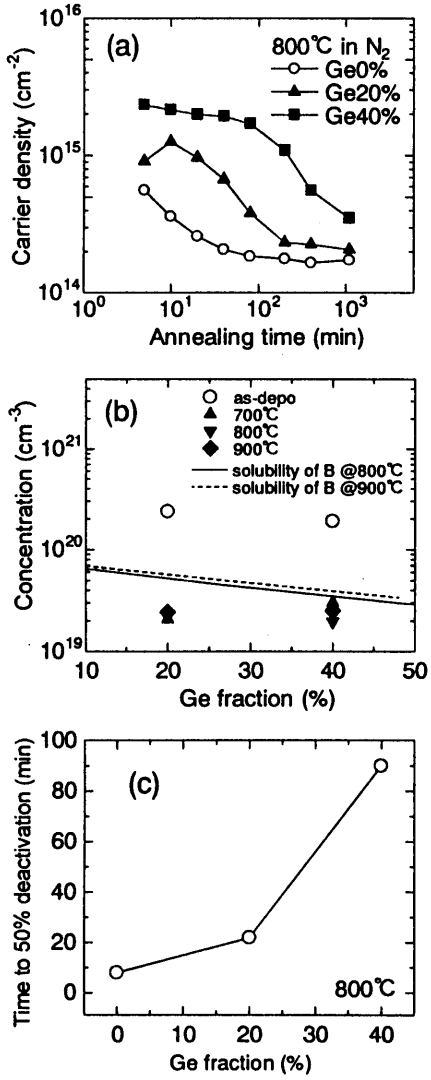

Fig.1 Isothermal annealing behaviors of carriers at 800°C (a) and Ge fraction dependence of carrier concentration for as-deposited and annealed ($\sim 10^3$ min) samples (b), and time to 50% deactivation (c). The solubility of B in poly-SiGe[9] are also shown in (b).

Figure 1(c) shows the annealing time at which 50% of the initial carriers were deactivated. The time to 50% deactivation markedly increases with increasing Ge fraction. This indicates that the thermal stability of substitutional B at the supersaturated concentration is significantly improved by Ge doping. For example, the stability for poly-$Si_{0.6}Ge_{0.4}$ is nine times as high as that for poly-Si.

Next, the deactivation process was analyzed. Figures 2(a) and 2(c) show semi-log plots of normalized change in the carrier concentration after annealing at 700 and 800°C, respectively. The change is normalized by the initial and final carrier concentrations. The deactivation characteristics in the initial stage are magnified in Figs. 2(b) and 2(d). It is found that the annealing characteristics consist of two linear parts, which suggests that the deactivation process consists of two first-order reactions with different time constants. Thus, the experimental data can be fitted to the following equation:

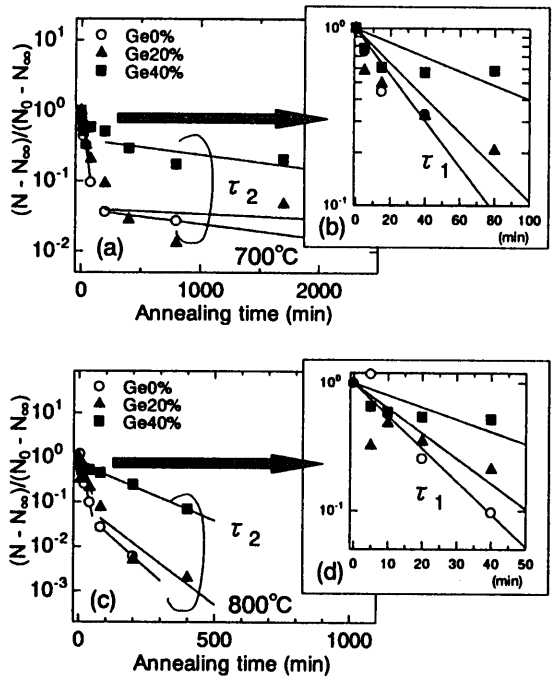

Fig.2 Isothermal annealing behaviors of normalized carrier concentration at 700 (a) and 800°C (c). The characteristics in the initial stage are magnified in (b) and (d).

$$\frac{N(t)-N_\infty}{N_0-N_\infty} = \Delta N_1 \exp(-t/\tau_1) + \Delta N_2 \exp(-t/\tau_2), \quad (1)$$

where $N(t)$, N_0, and N_∞ are carrier concentrations at t, $t=0$, and $t=\infty$, respectively, ΔN_1 and ΔN_2 are the carrier concentrations deactivated in the fast and slow processes, respectively, and τ_1 and τ_2 are the time constants for the fast and slow processes, respectively. The solid lines in the figures were obtained by fitting, and show good agreement with the experimental data.

Figure 3(a) shows the annealing temperature dependence of τ_2. It is found that τ_2 does not depend on the Ge fraction. From this Arrhenius plot, it is suggested that τ_2 can be fitted to the following equation:

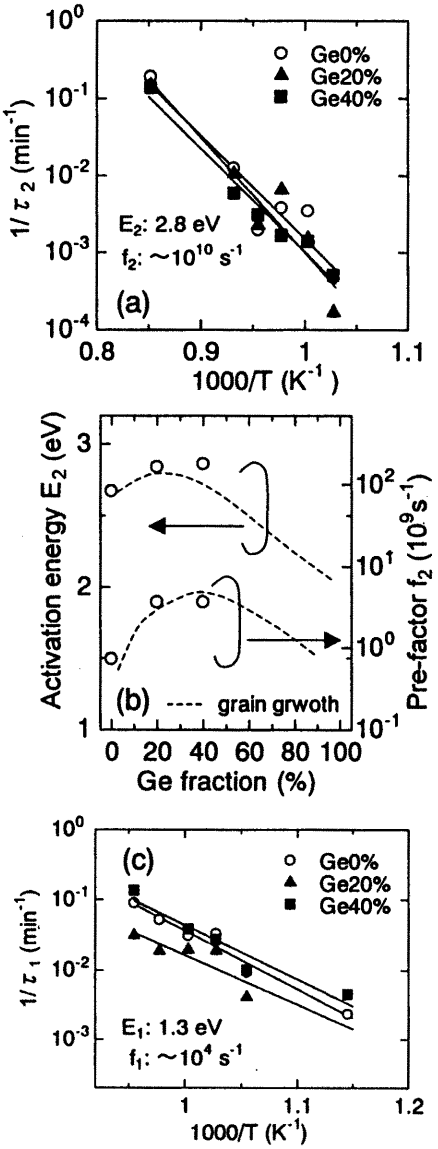

Fig.3 Arrhenius plot of τ_2 for slow process (a), Ge fraction dependence of activation energy and pre-exponential factor for τ_2 (b), and Arrhenius plot of τ_1 for fast process (c). The data of solid-phase growth of SiGe[10] are also shown in (b).

$$1/\tau_2 = f_2 \exp\left(-\frac{E_2}{kT}\right), \tag{2}$$

where f_2 and E_2 are the pre-exponential factor and activation energy, respectively, k is the Boltzmann constant, and T is the annealing temperature. By fitting to Eq. (2), an activation energy E_2 of 2.8 eV and pre-exponential factor f_2 of $\sim 10^{10}$ s^{-1} were obtained for all samples.

The activation energy and pre-exponential factor

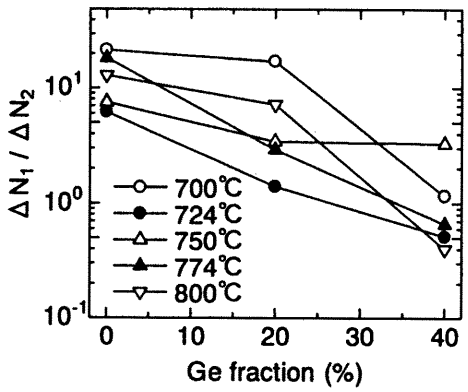

Fig.4 Ratio of concentration deactivated in fast process to that in slow process as a function of Ge fraction.

for the slow process are compared with those for solid-phase growth of SiGe[10] in Fig. 3(b). The parameters for the slow deactivation process of carriers show good agreement with those for solid-phase growth of SiGe. Moreover, grain growth under these annealing conditions was confirmed by TEM observation. These results clearly indicate that B deactivation in the slow process is related to grain growth of poly-SiGe. Thus, it can be concluded that B deactivation in the slow process is due to trapping of B at the grain boundaries during grain growth.

Figure 3(c) shows the Arrhenius plot of τ_1. The time constant for the fast process negligibly depends on the Ge fraction. The plot yields almost the same activation energy E_1 of 1.3 eV and pre-exponential factor f_1 of $\sim 10^4$ s^{-1} for all samples. Since deactivation of B atoms at supersaturated concentration should firstly be initiated by the movement of atoms, *i.e.*, from substitutional to interstitial sites, it is suggested that the fast process is due to the transition of sites of B atoms.

Thus, the fast and slow deactivation processes have been assigned to the two kinetics. However, the Ge fraction dependence of thermal stability shown in Fig. 1(c) cannot be explained by the analysis of $\tau_1(E_1, f_1)$ and $\tau_2(E_2, f_2)$.

In order to solve this problem, we focused on the ratio of carrier concentration deactivated in the fast and slow processes, *i.e.*, $\Delta N_1/\Delta N_2$. As shown in Fig. 4, with increasing Ge fraction, this ratio significantly decreases, and the slow deactivation process becomes dominant. Therefore, the thermal stability of B improves by Ge doping.

In order to understand these phenomena, we propose the two-state model as shown in Fig. 5: B

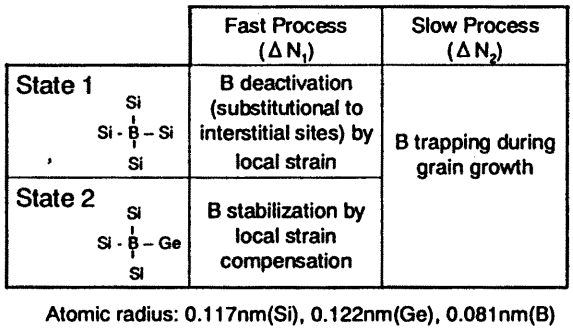

Fig.5 Two-state model for improvement of thermal stability of B by Ge doping.

atoms in poly-SiGe exist in two states, that is, B atoms surrounded by only Si atoms (state 1), and by Si and Ge atoms (state 2). In state 1, a local strain is induced due to the difference of atomic radii between Si and B atoms, so that B atoms are easily swept out from substitutional to interstitial sites. Such a local strain is compensated by Ge doping, because Ge atoms are larger than Si atoms. Thus, B atoms in state 2 are stable. Since stable B atoms (state 2) increase, the deactivated B atoms in the fast process (ΔN_1) decrease with increasing Ge fraction. It has been reported that diffusivity of B in epitaxial SiGe layers decreases with increasing Ge fraction[11),12),13),14)], which is attributed to atom-size misfit[14),15)]. The decrease in the diffusivity with increasing Ge fraction corresponds to the increase in thermal stability of B atoms. Thus, such reports support our model for the improvement in thermal stability of B atoms in the fast deactivation process.

On the other hand, the slow process (ΔN_2) is due to B trapping at grain boundaries, which is controlled by grain growth and is almost independent of Ge fraction. In this way, $\Delta N_1/\Delta N_2$ decreases with increasing Ge fraction. Therefore, thermal stability of B in poly-SiGe is improved by Ge doping.

4. Conclusion

Post-annealing characteristics of *in-situ* B-doped poly-SiGe have been investigated. Thermal stability of B is significantly improved by Ge doping, e.g., the stability for $Si_{0.6}Ge_{0.4}$ is nine times as high as that for Si. The deactivation process of B consists of the fast and slow processes. The time constants for both processes do not depend on the Ge fraction, while the ratio of deactivated B in the fast process to that in slow process decreases by Ge doping. The two-state model has been proposed, and explained the improved thermal stability of B by Ge doping.

Acknowledgments

This work was partially supported by a Grant-in-Aid for Scientific Research from the Ministry of Education, Culture, Sports, Science and Technology, and the 21st Century COE program.

References

1) T.-J. King, J. R. Pfiester, J. D. Shott, J. P. McVittie, and K. C. Saraswat, Int. Electron Devices Meet. Tech. Dig. (1990) 253.
2) T.-J. King, J. P. McVittie, K. C. Saraswat, and J. R. Pfiester, IEEE Trans. Electron Devices ED41 (1994) 228.
3) W.-C. Lee, Y.-C. King, T.-J. King, and C. Hu, IEEE Electron Device Lett. 19 (1998) 247.
4) M. Y. A. Yousif, M. Friesel, M. Willander, P. Lundgren, and M. Caymax, Solid-State Electron. 44 (2000) 1425.
5) Y. V. Ponomarev, P. A. Stolk, C. Salm, J. Schmitz, and P. H. Woerlee, IEEE Trans. Electron Devices ED47 (2000) 848.
6) F. N. Cubaynes, P. A. Stolk, J. Verhoeven, F. Roozeboom, and P. H. Woerlee, Mater. Sci. Semicond. Processing 4 (2001) 351.
7) Y. Yasuda, K. Hirabayashi, and T. Moriya, Supplement to Jpn. J. Appl. Phys. 43 (1974) 400.
8) B. S. Meyerson, F. K. LeGoues, T. N. Nguyen, and D. L. Harame, Appl. Phys. Lett. 50 (1987) 113.
9) P.-E. Hellberg, A. Ganor, S.-L. Zhang, and C. S. Petersson, J. Electrochem. Soc. 144 (1997) 3968.
10) P. Kringhøj, R. G. Elliman, M. Fyhn, S. Y. Shiryaev, and A. Nylandsted Larsen, Nucl. Instrum. Methods B 106 (1995) 346.
11) S. M. Hu, D. C. Ahlgren, P. A. Ronsheim, and J. O. Chu, Phys. Rev. Lett. 67 (1991) 1450.
12) N. Moriya, L. C. Feldman, H. S. Luftman, C. A. King, J. Bevk, and B. Freer, Phys. Rev. Lett. 71 (1993) 883.
13) G. H. Loechelt, G. Tam, J. W. Steele, L. K. Knoch, K. M. Klein, J. K. Watanabe, and J. W. Christiansen, J. Appl. Phys. 74 (1993) 5520.
14) P. Kuo, J. L. Hoyt, J. F. Gibbons, J. E. Turner, and D. Lefforge, Appl. Phys. Lett. 66 (1995) 580.
15) H.-J. Li, P. Kohli, S. Ganguly, T. A. Kirichenko, S. Banerjee, and P. Zeitzoff, Appl. Phys. Lett. 77 (2000) 2683.